Experimental Investigation of Curvature Effects on Ventilated Wall Jets

R. M. El-Taher*
King Abdulaziz University, Jeddah, Saudi Arabia

The results of an experimental study for a ventilated plane jet attaching to an offset plane surface or to an offset convex surface of circular cross section are presented. The results demonstrate the dependence of the rate of entrainment through the gap, the location of the attachment point, the growth of the length scale, and the decay of the maximum velocity on the wall curvature. Moreover, the effect of wall curvature on the mean velocity, the turbulence velocity components, and the Reynolds shear stress in the different zones of the jet are investigated.

Nomenclature

b = jet length scale (see Fig. 1)
h = jet offset distance
L = wall length (see Fig. 1)
P = static pressure
P_a = atmospheric pressure
P_N = stagnation pressure at nozzle exit
R = wall radius of curvature
r = radius of wall leading edge
Re = Reynolds number $= U_0 t/\nu$
t = jet nozzle thickness
U = mean velocity along the surface
U_m = jet local maximum velocity
U_0 = jet velocity at nozzle exit
U_s = entrained flow velocity through the gap
$\sqrt{\overline{u'^2}}$, $\sqrt{\overline{v'^2}}$ = root mean square of fluctuating velocity in x and y direction, respectively
x,y = distance measured along and normal to the surface, respectively
β = angle between flow direction at nozzle exit and flow direction at wall trailing edge
δ = y value where $U = U_m$
ρ = density
$\rho\overline{u'v'}$ = mean value of Reynolds shear stress
θ = wall deflection angle (see Fig. 1)
ν = kinematic viscosity

Introduction

JET attachment over adjacent walls can be separated into two classes. In the first class, there is no opening between the jet and the wall. This leads to the formation of a circulating flow region near the nozzle outlet, and a steplike flow exists. The second class is characterized by the existence of a gap between the jet and the wall, and a secondary flow is entrained through the gap, preventing the formation of the circulating region. The first class of jet attachment has several applications in fluidic industry. For example, the design of memory and other logic elements makes extensive use of this mode of attachment. The second class of jet attachment has wide applications in aircraft industry; for example, in powered high-lift systems of aircraft and in boundary-layer control devices.

Received Feb. 11, 1982; revision received Feb. 17, 1983.

*Associate Professor, Mechanical Engineering Department. Member AIAA.

The structure of the steplike wall jet (first class) has been studied by many investigators.[1-6] The second class of wall jet has recently received similar attention. Marsters[7,8] experimentally investigated the attachment of a ventilated plane jet on a parallel and on an inclined plane wall. His work was mainly concerned with the wall static pressure and mean velocity profiles. Shibil and Shaalan[9] experimentally investigated the attachment of a plane ventilated jet over a circular wall. They studied the effect of gap width and the angle of deflection of the wall on the wall pressure distribution, the rate of entrainment, and the position of point of attachment. Limited turbulence measurements were presented in that study. In an experimental investigation of a ventilated jet over parallel walls with relatively small gaps, El-Taher[10] found that the jet can be divided into the initial merging zone, the positive pressure gradient zone, the negative pressure gradient zone, and the fully developed zone. Within the last three zones, similarity of mean velocity, longitudinal turbulent velocity, transverse turbulent velocity and Reynolds shear stress profiles has been found. A detailed experimental study for the initial merging zone near the nozzle exit of a ventilated wall jet is described in Ref. 11. El-Taher[12] has also investigated the effect of surface roughness on the mean, as well as the turbulence, characteristics of ventilated wall jets.

The effect of curvature on turbulent wall jets has been investigated by many researchers in the last two decades.[13-23] These studies can be separated into two groups. The first group[13-20] is concerned with the development of jets around circular cylinders, and the second group[21-23] relates to flow

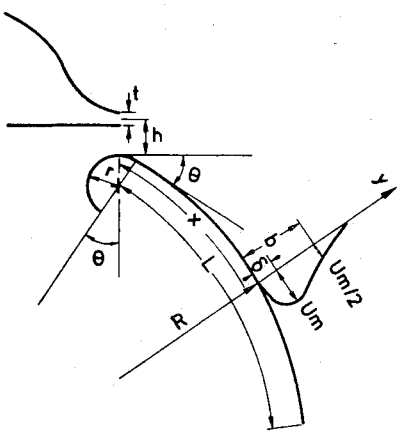

Fig. 1 Schematic diagram of flow of ventilated jet over circular arc.

around logarithmic spiral surfaces. However, the two groups are restricted to ordinary wall jets. With the exception of the work of Shibl and Shaalan,[9] who used a circular wall model with $R = 1400$ mm, it appears that no work is reported on the effect of curvature on ventilated wall jets. The work of Shibl and Shaalan was mainly devoted to the study of the mean flow characteristics. Limited turbulence data were presented in that work, and no comparison with the results for the flat wall or other values of wall curvature was undertaken. The present investigation, therefore, was intended to obtain a detailed insight into the effect of surface curvature on the mean, as well as the turbulence, characteristics of ventilated wall jets. Experiments were carried out for a two-dimensional ventilated turbulent jet attaching to a plane surface or to a circular convex surface. Turbulence measurements included logitudinal turbulence velocity $\sqrt{\overline{u'^2}}$, lateral turbulence velocity $\sqrt{\overline{v'^2}}$, and Reynolds shear stress $\overline{u'v'}$.

Experimental Arrangement

Figure 1 displays a sketch of the experimental arrangement. The nozzle block used in the present experiments is described elsewhere.[10] Four wall models with different surface curvatures were used. The models has identical leading edges (semicircle of 50 mm radius), and the length L of each model wall was 450 mm. The model walls were equipped with 0.5-mm-diam pressure taps distributed along the centerline of the surface at intervals of 12 mm. The walls were made to rotate about a center (0) to produce the required deflection angle θ. The wall-to-slot offset distance h as adjusted and measured using gage blocks. The range of the controlled variables is given in Table 1.

Hot wire traverses to measure mean velocity as well as the turbulence quantities $\sqrt{\overline{u'^2}}$, $\sqrt{\overline{v'^2}}$, and $\overline{u'v'}$ were carried out for the four model walls set at $h/t = 4$ and $\theta = 0$. Traverses were carried out at the midplane of each model at streamwise stations up to $150t$. The traverses followed a path normal to the wall at each station. Measurements were performed using an x-wire probe (DISA P63) and two DISA constant-temperature hot wire anemometers (55 M 10), along with linearizers, auxiliary units, and rms voltmeters for turbulence measurements. The turbulence intensity along the flow direction was also checked by a single hot wire probe. The probe was calibrated before and after each run to check for the repeatability of the calibration. No correction was applied to compensate for the assumption that the turbulent fluctuations are linear perturbations from the mean conditions.

Although it is recognized that Reynolds number effects are not negligible on curved wall jets,[19] the effect of Reynolds number was not explored in the present work. The experiments were carried out with the slot Reynolds number set at $Re = 1.48 \times 10^4$ with a slot width of 3 mm. The velocities at the nozzle outlet section were uniform over 85% of the slot width. The spanwise velocity distribution at the nozzle outlet section was found to be highly uniform, with a turbulence level of 0.22%.

The two-dimensionality of the flowfield was checked by measuring the lateral variation of the mean velocity at $x/t = 60$, at four different distances from the surface of the curved wall ($R = 300$). It was found that the variation in the mean velocity in the central half-width of the field was within $\pm 10\%$ from the centerline velocity. However, the variation near the side walls was less satisfactory, and velocities of as much as 25% higher than the centerline velocity were recorded in this region. However, it is well recognized that it is extremely difficult to obtain satisfactory two-dimensional curved flow,[23] and therefore the obtained degree of two-dimensionality was considered acceptable.

Experimental Results and Discussion

Wall Pressure Distribution

The wall static pressures were measured for each of the four model walls at the centerline of the surface, and no pressure measurements were performed in the spanwise direction. In every case the wall was set at four angles and several gap settings. The wall static pressure distribution for the different model walls at $\theta = 0$ and $h/t = 4$ are shown in Fig. 2, which is representative of all the data. The figure shows that the lowest subatmospheric pressure in the nozzle exit plane corresponds to the wall of highest curvature ($R = 300$), and the highest pressure corresponds to the flat wall ($R = \infty$). The static pressure distribution on the different model walls in the region, starting from the nozzle plane, are characterized by the three distinct zones observed by others.[7-10] These are the positive pressure gradient, the negative pressure gradient, and the constant pressure zones. The peak of the positive pressure corresponding to the flat wall ($R = \infty$) is higher than the peaks of the other three cases. The figure shows that while the pressure is atmospheric in the constant pressure zone of the flat wall, it is subatmospheric in the other cases of curved walls. As expected, the wall static pressure in the constant pressure zone decreases as the curvature increases due to the acceleration of the fluid particles in the direction normal to the wall. The shape of the pressure distributions shown in Fig. 2 indicates that there is a large pressure force on the curved walls compared to that on the flat wall. This force increases with the increase of wall curvature.

The decrease in surface pressure due to curvature increases the pumping action of the main jet to the secondary flow through the gap. This is effectively shown in Fig. 3, where the ratio U_s/U_0 is plotted against the deflection angle for the four model walls at $h/t = 4$. The velocity of the entrained flow was measured in the nozzle exit plane at y intervals of 1 mm by means of the hot wire. A slight nonuniformity was observed. In Fig. 3, U_s represents the mean velocity in the gap. Figure 3 also shows the results of Shibl and Shaalan.[9] The figure shows that the entrained flow velocity at a certain gap width increases with the deflection angle θ. The difference between the present results and the results of Ref. 9 may be attributed to two factors: 1) the Reynolds number in Ref. 9 was

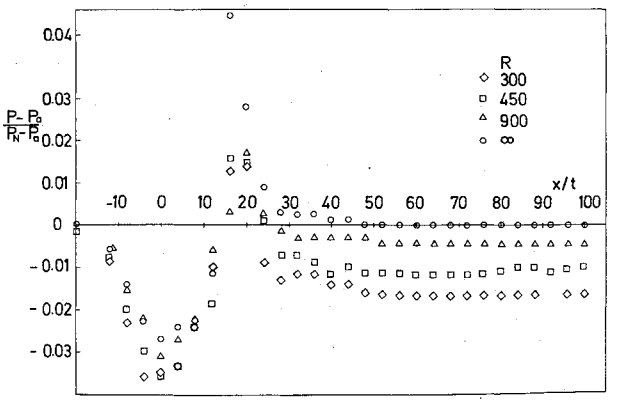

Fig. 2 Streamwise variation of surface pressure ($h/t = 4$, $\theta = 0$).

Table 1 Range of controlled variables

R, mm	300	450	900	∞
h/t	4, 6, 8, 10, 12	4, 6, 8, 10, 12	4, 6, 8, 10, 12	4, 6, 8, 10, 12
θ, deg	0, 15, 30, 45	0, 15, 30, 45	0, 15, 30, 45	0, 15, 30, 45

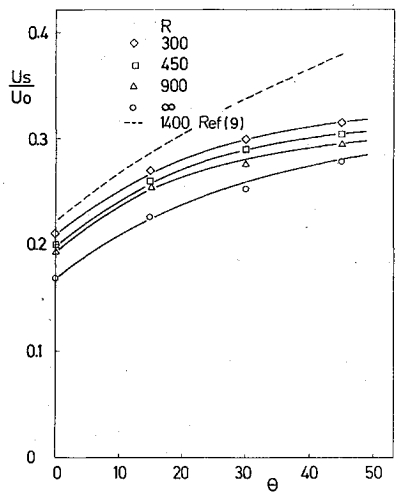

Fig. 3 Effect of surface curvature on entrainment velocity ($h/t=4$).

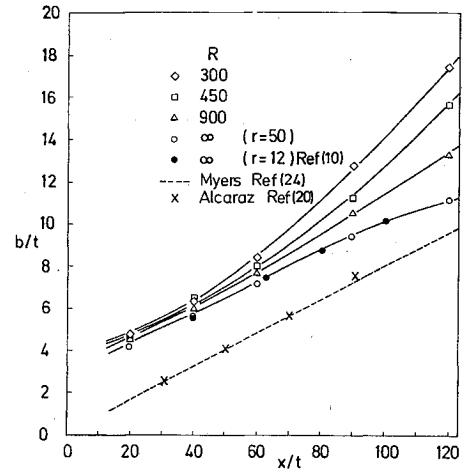

Fig. 5 Effect of curvature on the growth of jet length scale ($h/t=4$, $\theta=0$).

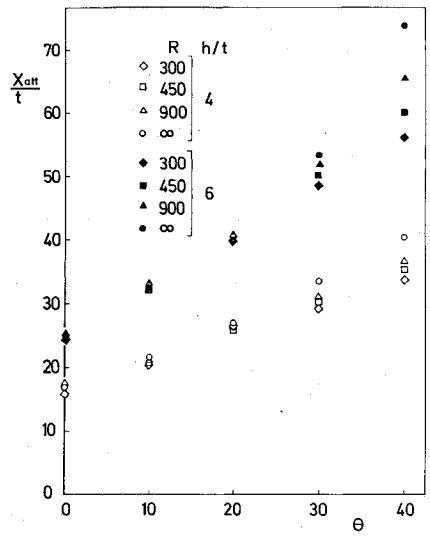

Fig. 4 Effect of curvature on position of attachment point.

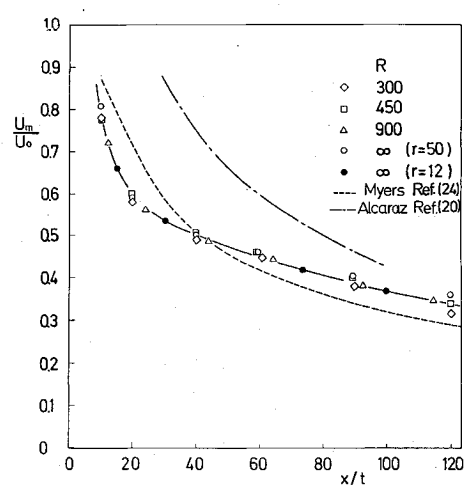

Fig. 6 Streamwise variation of maximum velocity ($h/t=4$, $\theta=0$).

2.33×10^4 compared to 1.48×10^4 in the present work; 2) the degree of the two-dimensionality of the flowfield in their experiments is expected to be different from that in the present work. Figure 3 clearly indicates the increase of flow entrainment through the gap due to wall curvature. For example, at $\theta=0$, $U_s/U_0=0.167$ for the flat wall ($R=\infty$), while $U_s/U_0=0.21$ for the curved wall of $R=300$. This represents a 25% increase in gap flow rate and a 58% increase in entrained momentum through the gap for the curved wall case.

Figure 4 shows the effect of surface curvature on the position of attachment point (maximum pressure point). The figure shows the location of the attachment point for different values of θ at two values of gap width ($h/t=4$ and 6) for the four model walls. The effect of curvature on the location of attachment point is more pronounced for $h/t=6$. The figure indicates that as the wall curvature increases, the attachment point gets closer to the nozzle mouth. This may be attributed to the decrease in the wall pressure and the corresponding increase in the curvature of the jet. This effect is less obvious at $\theta<20$ deg for these two values of h/t. However, it was found that the effect of curvature on the location of attachment point is more pronounced at larger values of h/t, even when the deflection angle θ was small.

Mean Velocity

Figure 5 shows the variation of the jet length scale in the streamwise direction for the different model walls at $\theta=0$ and $h/t=4$. The figure also shows the growth of the length scale of an ordinary wall jet along a flat wall[24] and along a convex circular wall of radius $R/t=322$ (Ref. 20). It is clear that the effect of the ventilating gap is to increase the jet width. This may be attributed to the entrained flow through the gap. The figure shows that the ventilated jet length scale b and its rate of growth in the streamwise direction db/dx increases with increasing of wall curvature. This was also observed by Sridhar and Tu[17] in their experimental study of curvature effects on ordinary wall jets and may be attributed to the effect of curvature on entrainment. However, it is worthwhile to note that the wall curvature in the experiments of Alcaraz et al.[20] is relatively small and has a negligible effect on the linear relation between b/t and x/t obtained by Myers et al.[24] for the plane wall jet.

The results of the flat wall of Ref. 10 are displayed in Fig. 5. The flat wall model of Ref. 10 has a circular leading edge of 12 mm radius in comparison with the 50 mm radius in the present experiments. It is clear that the wall leading edge radius has no effect on the length scale of the jet.

The streamwise decay of the jet maximum velocity is shown in Fig. 6 for the different model walls. The figure shows also the results of ordinary wall jets along a flat wall[24] and along a circular wall.[20] It can be readily noticed that surface curvature has a negligible effect on the decay of the velocity scale of the ventilated jet. It is remarkable that the present results are not far from Myers' results for ordinary wall jets. It is worthwhile to mention that the increase in the velocity scale in the results of Alcaraz as compared to Meyers' results is not due to wall

curvature, but is due to a difference in Reynolds number. The Reynolds number in Myers' experiments was 1.94×10^4, while it was 4×10^4 in the Alcaraz experiments. The experimental results of Guitton and Newman[23] for ordinary wall jets over convex surfaces having the shape of logarithmic spirals also indicated the weak dependence of the velocity scale on wall curvature. On the other hand, the results of Sridhar and Tu[17] for ordinary wall jets over circular surfaces showed that the velocity scale increases with an increase of surface curvature. However, it should be mentioned that the curvature of the wall models in the Sridhar and Tu experiments was comparatively large (values of R/t in their experiments were 6, 12, and 18 as compared to 100, 150, and 300 in the present experiments).

The effect of curvature on the location of maximum velocity point is shown in Fig. 7, where the resutls of Myers[24] and Alcaraz[20] for ordinary wall jets are also presented. The figure indicates that the thickness of the inner layer of ventilated jet is larger than the corresponding thickness for ordinary wall jets. This increase in thickness is due to the entrained flow through the gap. The figure also shows that the shift of the maximum velocity point away from the wall increases with an increase of wall curvature. This effect is more clearly seen in the constant pressure zone and may be attributed to the effect of curvature on the rate of entrainment.

The distribution of mean velocity in the outer layer of the constant pressure zone is shown in Fig. 8, where U/U_m is plotted vs $(y-\delta)/b$. It is clear that the velocity profiles are similar, and the similarity curve is not affected by curvature. The negligible effect of curvature on the nondimensional mean velocity profile in the outer layer of the jet was also observed by Sridhar and Tu[17] in the case of a conventional wall jet over convex circular walls. The solid line Fig. 8 represents the velocity distribution in the outer layer of an ordinary wall jet over a flat wall.[24] It is interesting that the profiles in the outer layer of the constant pressure zone are similar to those of ordinary wall jet.

The distribution of mean velocity in the inner region of the constant pressure zone is shown in Fig. 9. The figure shows the distribution of U/U_m vs y/δ for three cases of different wall curvatures. The velocity profiles collapse into a single curve in each case. However, there is a slight deviation between the similarity curves of the different wall models. This deviation may be attributed to the change of the radial pressure gradient with wall curvature and the corresponding effect on the mixing in the inner layer of the jet.

It was found that curvature had a negligible effect on the distribution of mean velocity in both the positive pressure gradient zone and the negative pressure gradient zone.

Turbulence Intensities and Shear Stress

Figure 10 shows the distribution of $\sqrt{u'^2}/U_0$ across the jet in the positive pressure gradient zone ($x/t=10$) and the negative pressure gradient zone ($x/t=20$). The results for the flat wall model ($R=\infty$) are compared with the results for the curved wall model of $R=300$ mm in this figure. The same general characteristics are observed in the two cases. Two turbulence peaks are observed in each case, with the larger peak lying in the outer layer. Also, the decrease of turbulence intensity in the streamwise direction is noticed in the two cases. The figure shows that curvature has no effect on the distribution of $\sqrt{u'^2}$ in the positive gradient zone ($x/t=10$). However, in the negative gradient zone ($x/t=20$), wall curvature is accompanied by an increase in $\sqrt{u'^2}$ in the outer layer and a slight decrease in the inner layer.

Experimental results showed that in the outer region of the negative pressure gradient zone, $\sqrt{v'^2}/U_m$ for $R=300$ is slightly larger than the corresponding value for $R=\infty$ (flat wall). However, it was found that the distribution of $\sqrt{v'^2}/U_m$ in the inner region is not affected by wall curvature.

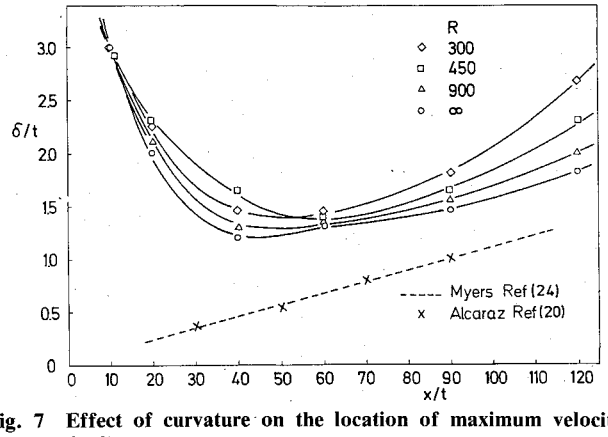

Fig. 7 Effect of curvature on the location of maximum velocity ($h/t=4, \theta=0$).

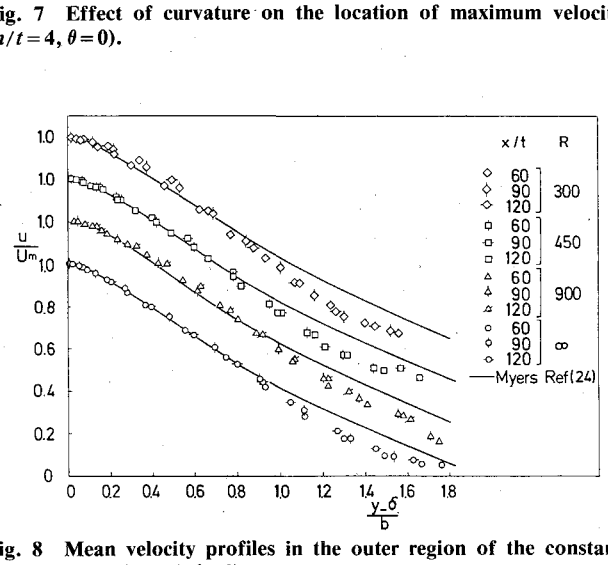

Fig. 8 Mean velocity profiles in the outer region of the constant pressure zone ($h/t=4, \theta=0$).

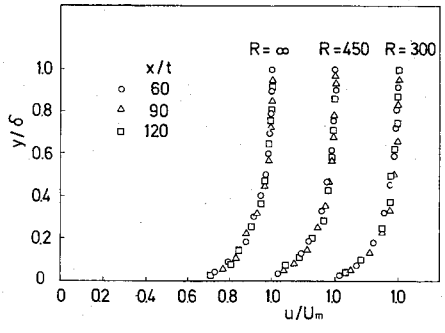

Fig. 9 Mean velocity profiles in the boundary-layer region of the constant pressure zone ($h/t=4, \theta=0$).

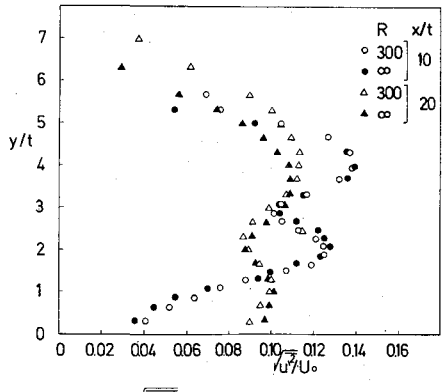

Fig. 10 Distribution of $\sqrt{u'^2}/U_0$ across the jet in the positive and negative pressure gradient zones ($h/t=4, \theta=0$).

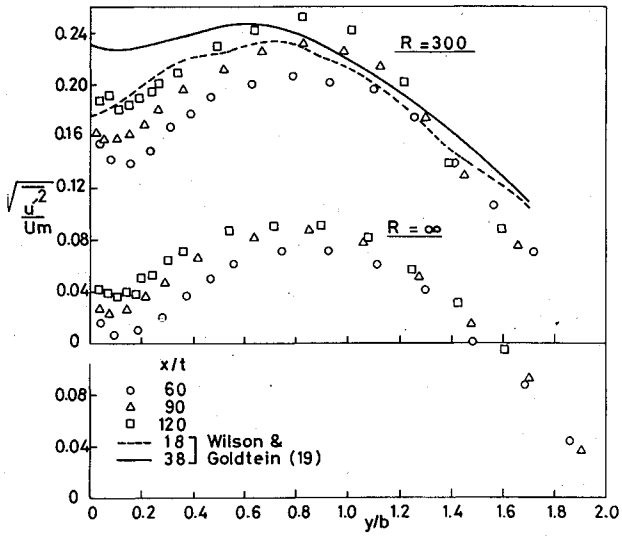

Fig. 11 Distribution of $\sqrt{u'^2}/U_m$ across the jet in the constant pressure zone ($h/t=4$, $\theta=0$).

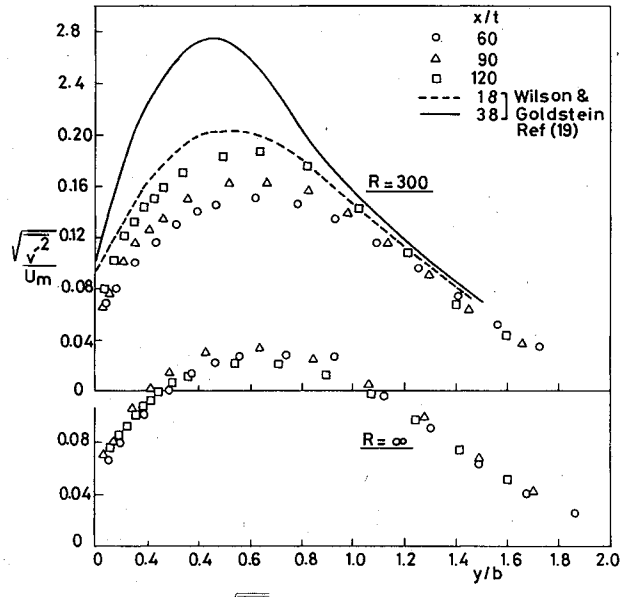

Fig. 12 Distribution of $\sqrt{v'^2}/U_m$ across the jet in constant pressure zone ($h/t=4$, $\theta=0$).

Similarly, it was found that the curvature has a negligible effect on the distribution of $\sqrt{v'^2}/U_m$ in the positive pressure gradient zone.

The distributions of $\sqrt{u'^2}/U_m$ and $\sqrt{v'^2}/U_m$ against y/δ in the constant pressure zone for $R=300$ and $R=\infty$ are shown in Figs. 11 and 12, respectively. The results of Wilson and Goldstein[19] are also displayed. The increase of the streamwise and cross-stream turbulence velocities due to wall curvature is readily noticed. However, it is remarkable that the increase in $\sqrt{v'^2}/U_m$ due to wall curvature is larger than the corresponding increase in $\sqrt{u'^2}/U_m$. For example, the percentage increase in the maximum value of $\sqrt{v'^2}/U_m$ at $x/t=120$ is 30%, whereas the corresponding increase in $\sqrt{v'^2}/U_m$ is only 17%. This is, however, expected, since it is noticed from Fig. 5 that the rate of spreading of the wall jet increases with an increase of wall curvature and, since it is the y-direction fluctuations that are instrumental in transferring momentum, the increase in $\sqrt{v'^2}$ can be intuitively predicted to be larger than the corresponding increase in $\sqrt{u'^2}$.

Figures 11 and 12 show that in the case of the curved wall ($R=300$), both $\sqrt{u'^2}$ and $\sqrt{v'^2}$ display a similar increase in their maximum values, between 60 and 120 slot heights, of about 26%. The results of Wilson and Goldstein[19] exhibit a rather different evolution. The streamwise turbulence velocity component shows little variation between $x/t=18$ and 38, whereas the radial component displays a 35% augmentation. The main reason for the different developments in the present experiments and the Wilson and Goldstein experiments[19] is probably due to the difference in R/t: In the present work, $R/t=100$, while in their work, $R/t=16.8$. The fluctuating pressure reflections from the wall act as an important damper of the radial velocity fluctuations, since they hinder the transfer of energy from u'^2 to v'^2; their influence is fundamental in making v'^2 in the plane wall jet so much smaller than in the free jet. The wall radius in the Wilson and Goldstein experiments is much smaller than the radius in the present work, and it seems intuitive that the wall-reflection mechanism will be less effective in impeding the transfer of energy than in the present work.

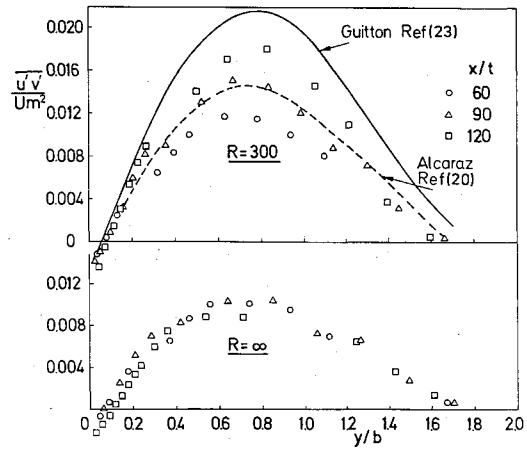

Fig. 13 Distribution of shear stress across the jet in the constant pressure zone ($h/t=4$, $\theta=0$).

Figure 13 shows the effect of wall curvature on the shear stress distribution in the constant pressure zone. The figure shows the distribution of $\overline{u'v'}/U_m^2$ against y/b for different values of x/t at $R=300$ and ∞. The solid line on Fig. 13 represents the measurements of Guitton and Newman[23] for a wall jet over a logarithmic spiral ($x/R=\frac{2}{3}$), while the dashed line represents the mean curve through the experimental results of Alcaraz et al.[20] The increase in the magnitude of $\overline{u'v'}$ as a result of wall curvature is readily noticed in the figure. It is seen that while the data of the flat wall ($R=\infty$) collapse into a single mean curve, the normalized shear stress for the curved wall ($R=300$) increases as the flow develops along the wall. For example, the maximum value of $\overline{u'v'}/U_m^2$ increases from 0.012 to 0.018 as the flow develops along the curved wall between $x/t=60$ and 120. This is consistent with the mean flow characteristics shown in Fig. 5. It is seen from Fig. 5 that the rate of the growth of the jet at $R=\infty$ is essentially invariant with x; correspondingly, the normalized shear stress profiles are nearly the same at different streamwise stations. On the other hand, Fig. 5 shows that the growth rate of the jet at $R=300$ starts at the flat-wall value, but rises by some 200% at $x/t=120$; correspondingly, the normalized turbulent shear stress progressively increases with increase of x. The results of Alcaraz[20] at $Re=4.0\times10^4$ showed a similar increase in $\overline{u'v'}$ along the wall. In that case, the maximum turbulent shear stress $\overline{u'v'}/U_m^2$ increases from 0.012 to 0.017 as the jet develops along the wall. The agreement between the present results and those of Alcaraz et al., though wall curvatures are different, may be attributed to the different values of the Reynolds number and the different degrees of flow two-dimensionality in the two sets of experiments.

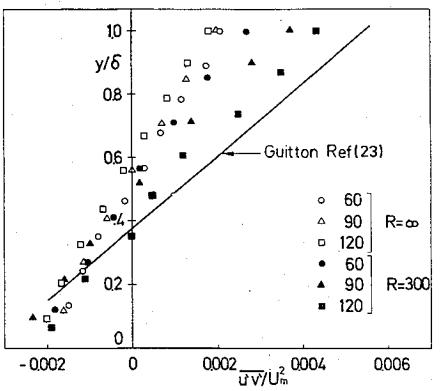

Fig. 14 Distribution of shear stress in the boundary layer of the constant pressure zone ($h/t=4$, $\theta=0$).

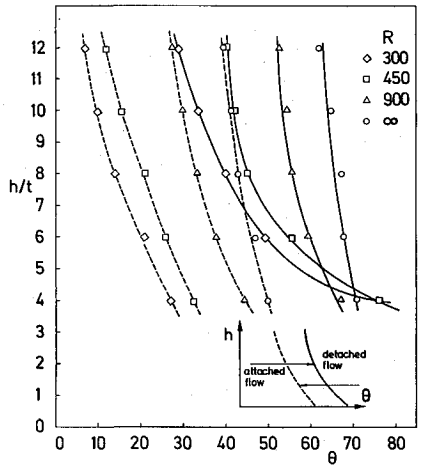

Fig. 15 Effect of curvature on attachment limits.

Figure 14 shows the distribution of the turbulent shear stress plotted against y/δ in the inner region of the constant pressure zone for $R=300$ and $R=\infty$. The increase in the turbulent shear stress in the inner region due to wall curvature is readily noticed. The figures shows that the shear stress profiles are similar in the case of the flat wall, whereas the normalized shear stress increases as the flow develops along the curved wall. It is seen from the figure that the shearing stress remains positive in this region for both $R=300$ and $R=\infty$ even though $\partial U/\partial y$ becomes positive. It is interesting to note that the position of zero shear stress gets closer to the surface as the flow develops along the curved wall. For example, the position of zero shear stress is shifted from $y/\delta=0.5$ to 0.36 as the flow develops between $x/t=60$ and 120. The corresponding position for the flat wall is nearly fixed at $y/\delta=0.55$.

Effect of Curvature on Attachment Limits

The limiting values of gap size and deflection angle were obtained by observing the flow pattern on the surface by means of fine threads stuck to the trailing edge of the model walls. The limiting value of the deflection angle was obtained first by gradually increasing the deflection angle until the threads indicated the occurrence of flow detachment. Then the deflection angle was gradually decreased until attached flow was regained. The limiting values of h and θ are shown in Fig. 15. It is seen that for a certain gap width h, the limiting value of θ for attached flow decreases with an increase of wall curvature. Likewise, the limiting value of θ for detached flow decreases with an increase of curvature. Although the limiting wall angle for attached flow at a certain gap width decreases with an increase of wall curvature, the corresponding limiting jet deflection angle β increases. For example, Fig. 15 indicates that at $h/t=6$ the limiting wall angle θ for attached flow is 68 deg for a flat wall ($R=\infty$) and is 48 deg for a curved wall ($R=300$). However, it was found that the corresponding jet deflection angles are 68 and 135 deg, respectively.

Conclusions

This experimental investigation has provided fairly detailed measurements of the effect of wall curvature on the mean velocity field, as well as the turbulence characteristics of ventilated wall jets. The following conclusions are drawn from this work:

1) The rate of entrainment through the gap increases as the surface curvature increases. Moreover, the attachment point gets closer to the nozzle mouth with an increase of wall curvature. The attachment and detachment limiting wall deflection angles at a certain gap width decrease with an increase of wall curvature. However, the limiting jet deflection angle increases with increasing wall curvature.

2) Wall curvature has a negligible effect on the flowfield in the positive and negative pressure gradient zones.

3) The rate of growth of the length scale in the streamwise direction increases with an increase of wall curvature, and values for db/dx as much as 200% higher than that of the flat wall value were recorded in the constant pressure zone for $R=300$. However, it was found that curvature has a negligible effect on the decay of mean velocity scale.

4) Similarity of mean velocity profiles in the outer layer of the constant pressure zone is not affected by wall curvature, whereas the similarity curve in the inner layer appears to change slightly with increasing curvature.

5) The most important effect of curvature on turbulence in the constant pressure zone is an increase of $\sqrt{u'^2}$, $\sqrt{v'^2}$, and $u'v'$. The increase in $\sqrt{v'^2}$ due to wall curvature is much larger than the corresponding increase in $\sqrt{u'^2}$. The shear stress at the maximum velocity is larger and is of the same sign as the shear stress in the outer region of the constant pressure zone for both flat and curved walls.

References

[1] Bourque, C. and Newman, B. G., "Reattachment of a Two-Dimensional Incompressible Jet to an Adjacent Flat Plate," *Aeronautical Quarterly*, Vol. 11, Aug. 1960, pp. 201-232.

[2] Sawyer, R. A., "Two-Dimensional Reattaching Jet Flows Including the Effect of Curvature on Entrainment," *Journal of Fluid Mechanics*, Vol. 17, Dec. 1963, pp. 481-498.

[3] Kumada, M., Mabuchi, I., and Oyakawa, K., "Studies in Heat Transfer to Turbulent Jets with Adjacent Boundaries," 3rd Report, *Bulletin of the JSME*, Vol. 16, Nov. 1973, pp. 1712-1722.

[4] Ayukawa, K. and Shakouchi, T., "Analysis of a Jet Attaching to an Offset Parallel Plate," *Bulletin of the JSME*, Vol. 19, April 1976, pp. 395-401.

[5] Parameswaran, V. and Alpay, S. A., "Studies on Reattaching Wall Jets," *Transactions of the CSME*, Vol. 3, No. 2, 1975, pp. 83-94.

[6] Hoch, J. and Jiji, L. M., "Two-Dimensional Turbulent Offset Jet-Boundary Interaction," *Journal of Fluids Engineering*, Vol. 103, March 1981, pp. 154-161.

[7] Marsters, G. F., "The Attachment of a Plane Ventilated Jet to a Plane Parallel Wall," *Transactions of the CSME*, Vol. 4, No. 4, 1976-77, pp. 197-203.

[8] Marsters, G. F., "The Attachment of a Ventilated Plane Jet to an Inclined Plane Wall," *Aeronautical Quarterly*, Vol. 29, May 1978, pp. 60-72.

[9] Shibl, A. and Shaalan, M., "Turbulent Jet Attachment Over a Circular Wall," Paper 80-C2/Aero-2, ASME, Century 2 Aerospace Conference, San Fransisco, Calif., Aug. 13-15, 1980.

[10] El-Taher, R. M., "Similarity in Ventilated Wall Jets," *AIAA Journal*, Vol. 20, Feb. 1982, pp. 161-166.

[11] El-Taher, R. M., "Experimental Study of the Flow Fluid Near the Nozzle in Ventilated Wall Jet," *Journal of Engineering and Applied Sciences*, Vol. 1, No. 3, 1981, pp. 211-221.

[12] El-Taher, R. M., "Attachment of Ventilated Jets to Rough Boundaries," *The Aeronautical Journal of the Royal Aeronautical Society*, Vol. 86, Dec. 1982, pp. 380-383.

[13]Newman, B. G., "The Deflection of Plane Jets by Adjacent Boundaries-Coanda Effect," *Boundary Layer and Flow Control*, Pergamon Press, London, 1961.

[14]Nakaguchi, H., "Jet Along a Curved Wall," Dept. of Aeronautics, University of Tokyo, Tokyo, Japan, Research Memo No. 4, 1961.

[15]Fekete, G. I., "Coanda Flow in a Two-Dimensional Wall Jet on the Outside of a Circular Cylinder," Mechanical Engineering Dept., McGill University, Rept. No. 63-11, 1963.

[16]Guitton, D. E., "Two-Dimensional Wall Jets Over Curved Surfaces," Mechanical Engineering Dept. Rept. No. 64-7, McGill University, Montreal, Canada, 1964.

[17]Sridhar, K,. and Tu, P.K.C., "Experimental Investigation of Curvature Effects on Turbulent Wall Jets," *The Aeronautical Journal of the Royal Aeronautical Society*, Vol. 73, Nov. 1969, pp. 977-981.

[18]Wilson, D. J., "An Experimental Investigation of the Mean Velocity, Temperature and Turbulence Fields in Plane and Curved Two-Dimensional Wall Jets: Coanda Effect," Ph.D. Thesis, Mechanical Engineering Dept., University of Minnesota, 1970.

[19]Wilson, D. J. and Goldstein, R. J., "Turbulent Wall Jets with Cylindrical Streamwise Surface Curvature," *Journal of Fluids Engineering*, Vol. 98, Sept. 1976, pp. 550-557.

[20]Alcaraz, E., Charnay, G., and Mathieu, J., "Measurements in a Wall Jet Over a Convex Surface," *The Physics of Fluids*, Vol. 20, No. 2, 1977, pp. 203-210.

[21]Sawyer, R. A., "Two-Dimensional Turbulent Jets with Adjacent Boundaries," Ph.D. Thesis, Cambridge University, Cambridge, England, 1962.

[22]Guitton, D. E., "Some Contributions to the Study of Equilibrium and Nonequilibrium Wall Jets Over Curved Surfaces," Ph.D. Thesis, McGill University, Montreal, Canada, 1968.

[23]Guitton, D. E. and Newman, B. G., "Self-Preserving Turbulent Wall Jets Over Convex Surfaces," *Journal of Fluid Mechanics*, Vol. 81, Pt. 1, 1977, pp. 155-185.

[24]Myers, G. E., Schaur, J. J., and Eustis, R. H., "The Plane Turbulent Wall Jet," Stanford University, Stanford, Calif., Technical Rept. No. 1, 1961.